Electronic Supplementary Material (ESI) for ChemComm.

Supporting Information to

Unexpected arene ligand exchange results in the oxidation of an organoruthenium anticancer agent: the first X-ray structure of a protein–Ru(carbene) adduct

Matthew P. Sullivan,[a,b] Michél K. Nieuwoudt,[a,c] Graham A. Bowmaker,[a] Dianna Truong,[a] Nelson Y. S. Lam,[a] David C. Goldstone,*[b] and Christian G. Hartinger*[a]

[a] *School of Chemical Sciences, University of Auckland, Private Bag 92019, Auckland 1142, New Zealand.*

[b] *School of Biological Sciences, University of Auckland, Private Bag 92019, Auckland 1142, New Zealand.*

[c] *The Photon Factory, University of Auckland, New Zealand*

Table of Contents

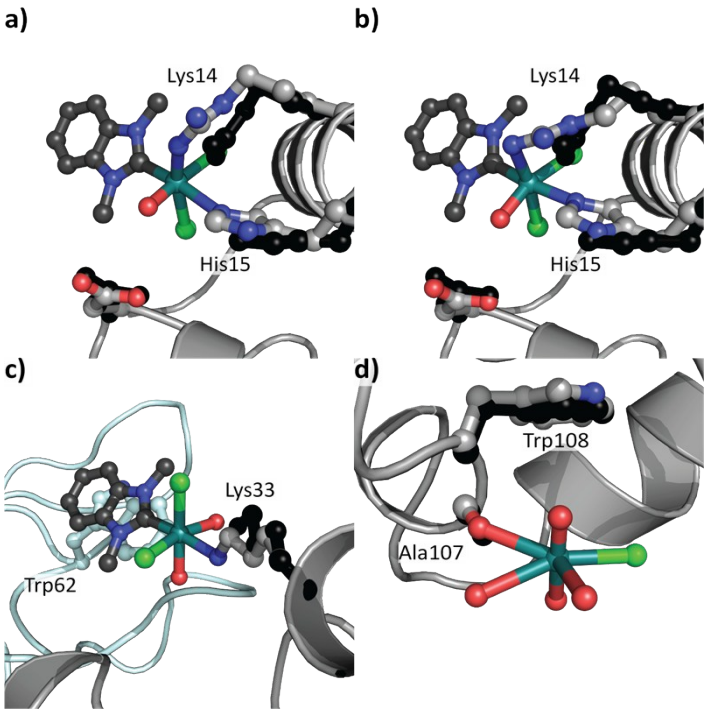

Figure S1. Ru binding sites I and II as results from the reaction between HEWL and **1** overlaid with the native structure of HEWL (PDB ID 4NHI) shown in black. a) After 3 d (PDB ID 6BO1) and b) 1 month (PDB ID 6BO2) incubation periods, the positions of the residues Arg14 and His15 change as compared to the HEWL structure. c) Structural alteration of the Lys33 residue after 1 month of soaking and featuring the [Ru(1,3-dimethylbenzimidazol-2-ylidene)$(OH_x)_2Cl_2$] adduct. The adjacent asymmetric unit is shown as a light teal cartoon in the background. d) Positional change of Trp108 after 1 month of soaking.

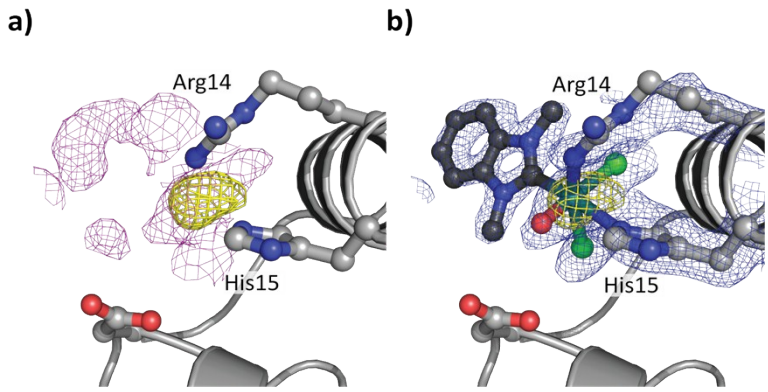

Figure S2 Details of binding site I for 1 on HEWL after 3 d incubation. The [Ru(dmb)(OH_x)Cl_2] moiety is indicated in ball and stick representation with the Ru in teal. The electron density maps are contoured at 1σ (magenta and blue maps) while the anomalous difference maps are contoured at 4σ (yellow maps). a) Unbiased electron density (magenta) and anomalous difference map showing the site of interaction. b) Placement of the [Ru(dmb)(OH_x)Cl_2] fragment into the refined electron density map (blue) with anomalous difference map, showing the bidentate modality of the interaction.

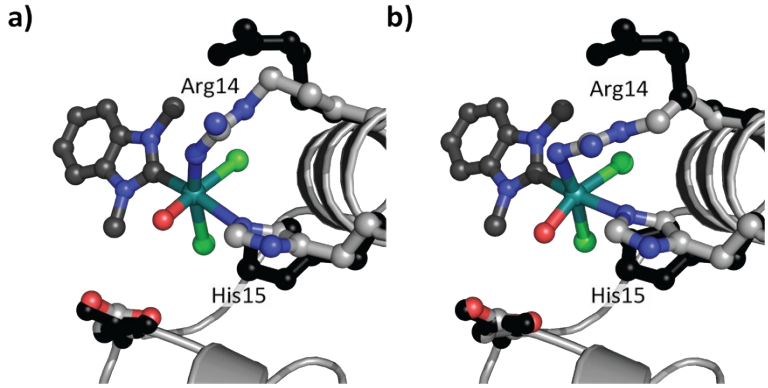

Figure S3. Ru binding sites as results from the reaction between HEWL and **1** and overlaid with the HEWL–Ru(η^6-*p*-cymene)Cl_2 structure (PDB ID 5V4G) shown in black, highlighting the positional change of Arg14 after a) 3 d and b) 1 month soaking periods.

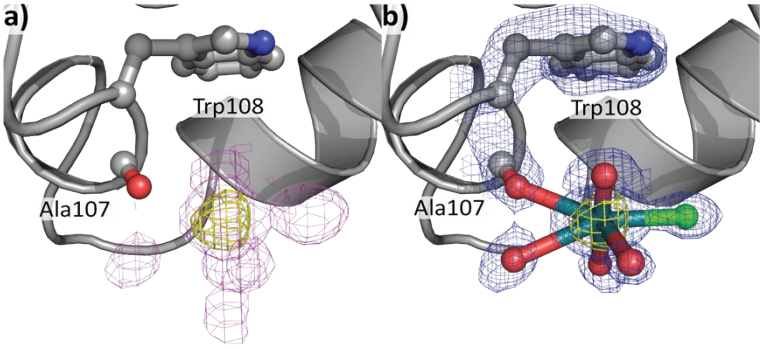

Figure S4. Details of binding site III detected in the HEWL structure soaked for 1 month with **1** showing a Ru ion sitting in the solvent channel. The Ru was identified to interact with the carbonyl O atom of Ala107. The electron density maps are contoured at 1σ (magenta and blue maps) while the anomalous difference maps are contoured at 4σ (yellow maps). a) Unbiased electron density (magenta) and anomalous difference map (yellow) showing the site of interaction. b) Placement of a $[RuCl(OH_x)_4]$ fragment into the refined electron density map (blue) with anomalous difference map, showing the monodentate coordination mode.

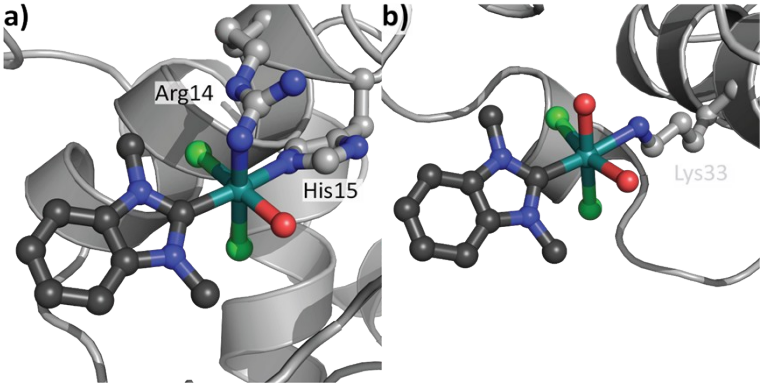

Figure S5. Illustration of the octahedral Ru(NHC) adducts interacting with HEWL a) at site I through bidentate coordination involving Arg14 and His15, and b) at site II through monodentate coordination at Lys33.

To further support the positioning of the organometallic moieties, maps were generated using phenix.polder,[1] which allow for weak ligand density to be viewed in sharper detail (Fig. S4) and simulated annealing composite omit maps, which further proved the ligand identity (Fig. S5).[2]

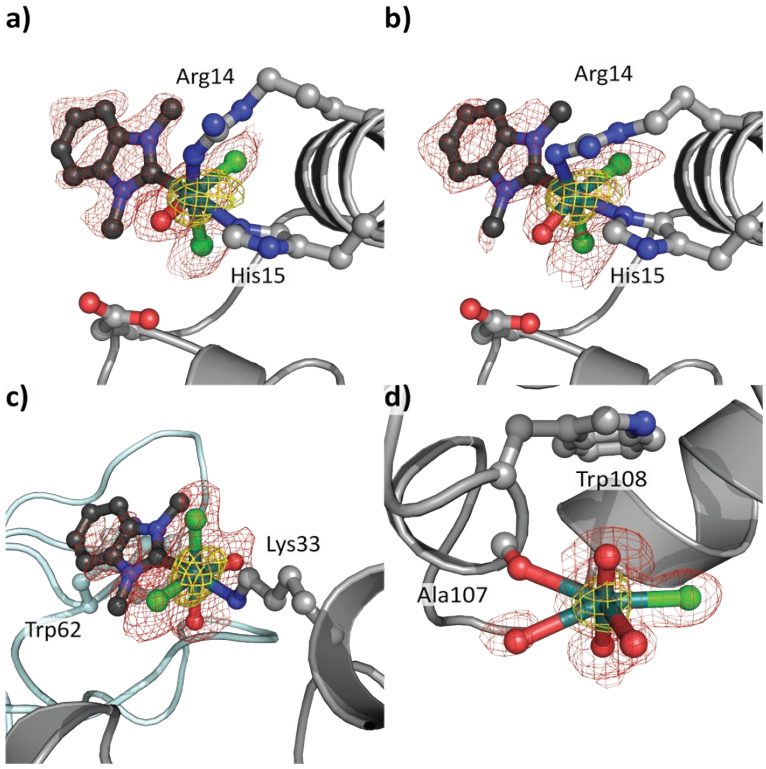

Figure S6. Ru binding sites I and II with a map generated by phenix.polder which allows for ligand densities to be displayed with the exclusion of bulk solvent. a) For the crystal data resulting from a 3 d soak, a polder map was generated which was contoured to 3σ about the metal fragment [Ru(1,3-dimethylbenzimidazol-2-ylidene)(OH_x)Cl_2] with Arg14 and His15 shown as a reference. b) For the structural data collected after 1 month of soaking a HEWL crystal with **1**, a polder map was generated which was contoured to 2σ about the [Ru(1,3-dimethylbenzimidazol-2-ylidene)(OH_x)Cl_2] moiety with Arg14 and His15 shown as a reference. c) Polder map for crystal data for a 1 month soak contoured to 2σ about the [Ru(1,3-dimethylbenzimidazol-2-ylidene)(OH_x)$_2Cl_2$] ligand with Lys33 shown as a reference, while the adjacent asymmetric unit with Trp62 is given in light teal. d) Polder map contoured to 2σ about the [RuCl(OH_x)$_4$] moiety with Trp108 shown as a reference after soaking HEWL with **1** for 1 month.

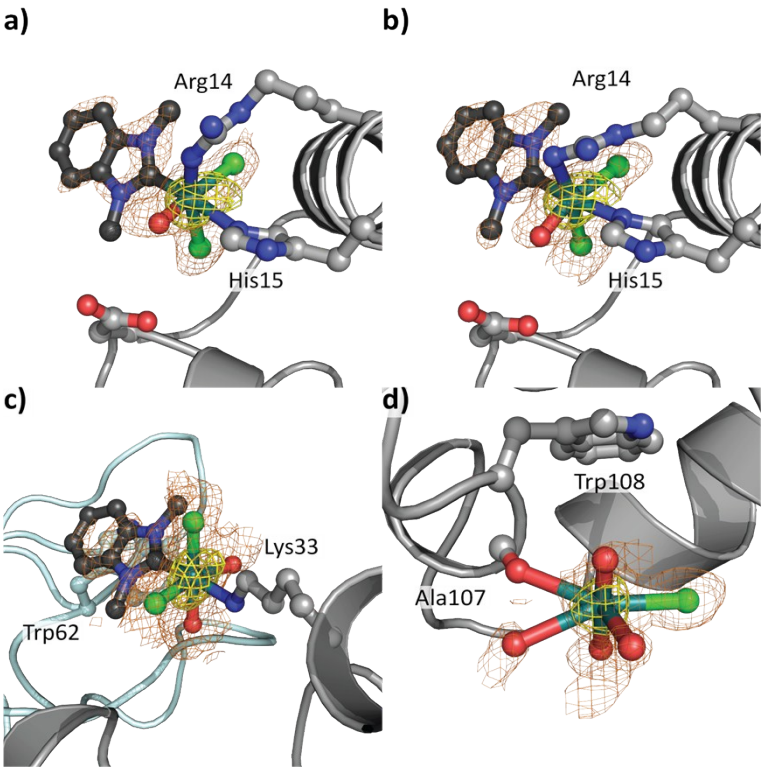

Figure S7. Ru binding sites with maps generated by simulated annealing composite omit which validates the density surrounding the ligand. a) For the crystal data resulting from a 3 d soak, a simulated annealing composite omit map was generated which was contoured to 3σ about the metal fragment [Ru(1,3-dimethylbenzimidazol-2-ylidene)(OH_x)Cl_2] with Arg14 and His15 shown as a reference. b) For the structural data collected after 1 month of soaking a HEWL crystal with **1**, a simulated annealing composite omit map was generated which was contoured to 2σ about the [Ru(1,3-dimethylbenzimidazol-2-ylidene)(OH_x)Cl_2] moiety with Arg14 and His15 shown as a reference. c) Simulated annealing composite omit map for crystal data for a 1 month soak contoured to 2σ about the [Ru(1,3-dimethylbenzimidazol-2-ylidene)(OH_x)$_2Cl_2$] ligand with Lys33 shown as a reference, while the adjacent asymmetric unit with Trp62 is given in light teal. d) Simulated annealing composite omit map contoured to 2σ about the [RuCl(OH_x)$_4$] moiety with Trp108 shown as a reference after soaking HEWL with **1** for 1 month.

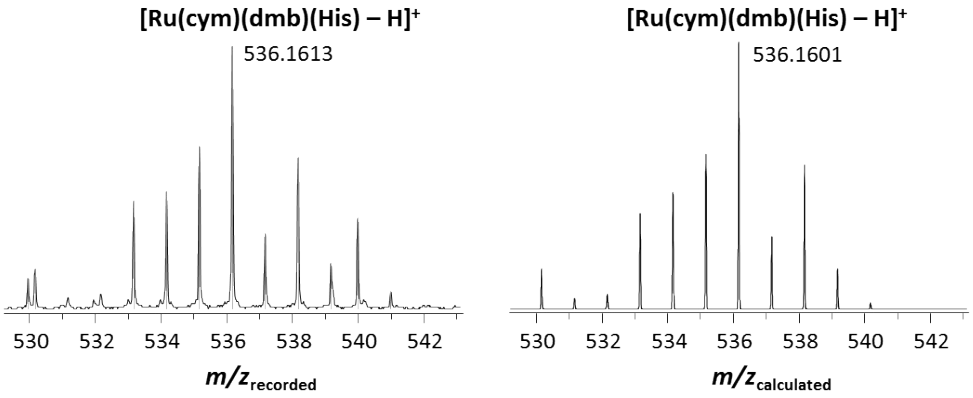

Figure S8. Mass spectrometric investigation of the binding of **1** to His. Zoom into the recorded spectrum for the His adduct $[Ru(cym)(dmb)(His) - H]^+$ and the calculated isotope pattern for the same peak.

Experimental

Synthesis

Compound **1** was prepared using the synthetic method described by Ott *et al*.[3]

Protein crystallography

HEWL crystals of 0.1–0.2 mm were grown from a reservoir solution consisting of NaCl (0.8 M) and NaOAc (0.1 M, pH 4.7) which in the crystallisation drop was mixed with an equal volume of HEWL (100 mg/ml).[4] Crystals formed within 24 h, and were then transferred into a drop of reservoir solution of $NaNO_3$ (0.8 M) and NaOAc (0.1 M, pH 4.7) supplemented with **1** (1.04 mg, 1 mg/mL). The crystals were observed to turn orange after 3 d, and X-ray analysis was performed after a period of 3 d and 1 month. For this purpose, the soaked crystals were transferred into a cryoprotectant of 20% glycerol, $NaNO_3$ (0.8 M) and NaOAc (0.1 M, pH 4.7), and flash frozen in liquid nitrogen.

Crystal data collection and analysis

X-ray diffraction data were collected on the crystallography beamlines MX1 at the Australian Synchrotron.[5] Data were processed with XDS.[6] The protein crystallised in the space group $P4_32_12$. The structures were determined by molecular replacement using a monomer of lysozyme (PDB ID 4NHI) as a search model in PHASER.[7] The models were refined with iterative rounds of refinement and model building in REFMAC[8] and COOT.[9] Sodium ion placement was aided by the use of the WASP server at USF.[10] The anomalous difference maps were generated using FFT.[11] The fragment formed was reformatted using Gaussian[12] (from the small molecule crystal structure of **1**), while the final PDB and CIF files were generated by phenix.elbow.[13]

Electron paramagnetic resonance

HEWL crystallisation was performed in EPR tubes (Wilmad 730-SQ-250M, 5 mm outer diameter) by mixing HEWL (1.25 ml, 100 mg/mL) and a crystallisation solution (0.7 M NaCl and 1.25 ml of 0.1 M NaOAc pH 4.7). The batch crystallization was performed over a period of 3 days, with crystals settling in the base of the EPR tube. The solution above the crystals was removed and

the protein concentration was determined as 6.51 mg/mL using the molar absorptivity of HEWL and absorbance at 280 nm. The crystals were washed with the soaking buffer (0.7 M $NaNO_3$ and 0.1 M NaOAc pH 4.7) and left overnight. The protein concentration was again measured and determined to be 1.27 mg/mL. The crystals were soaked with **1** (3.95 mg in 2.50 mL H_2O, 3.49 mM) or indazolium [*trans*-tetrachloridobis(indazole)ruthenate(III)] (KP1019) (5.22 mg in 2.50 mL H_2O, 3.49 mM) in the soaking buffer (0.7 M $NaNO_3$, 0.1 M NaOAc, pH 4.7) for a period of 6 d, resulting in partial dissolution of the crystals.

EPR spectra were recorded using X band frequencies in a TE011 cavity of a JEOL JES-FA-200 spectrometer equipped with a variable temperature controller. Samples were cooled to 123 K and spectra were recorded at 9095.8 MHz with 100 kHz modulation, and 20 mW. Spectra of the buffer, and of crystals of HEWL and **1**, as well as the control, KP1019, were recorded under the same conditions. Five spectra of the conjugate HEWL–**1** were recorded and then co-added to improve the signal-to-noise ratio. Calculation of the integrated area for this spectrum was then divided by 5 for comparison of number of spins with the HEWL–KP1019 conjugate. The number of spins was calculated using the area obtained by doubly integrating the 1st-derivative EPR spectrum

$$N_{sample} = \frac{Area_{sample}}{Area_{CuSO_4}} \times n(CuSO_4) \times 6.02 \times 10^{23} \qquad \text{eq. S1}$$

where n = number of moles of $CuSO_4$ standard measured. The $CuSO_4$ spectrum was recorded at the same conditions except at one third of the gain; its integrated area was thus tripled to adjust for accurate calculation.

The spectra were simulated using the JEOL anisotropic simulation software. The HEWL–KP1019 spectrum is complex, showing more than one anisotropic signal. The g value range (axial and rhombic species g = 0.95–3.08) was consistent with those observed for KP1019 in other environments, as is the presence of more than one Ru^{III} signal.[14]

Table S1. Simulation parameters for HEWL–**1** using species HEWL–**1a**, HEWL–**1b**, and HEWL–**1c**.

Parameter	HEWL–**1a**	HEWL–**1b**	HEWL–**1c**
Intensity	86	36	250
# electron spins	½	½	½
g_x	2.18	2.52	3.08
g_y	2.14	2.38	2.24
g_z	2.00	1.91	1.77
S_x	8	22	45
S_y	18	22	33
S_z	40	23	38

Mass spectrometry

Binding studies between **1** and His or HEWL were conducted with ESI-MS. His (1 mM) and **1** (1 : 1) were incubated at 25 °C for 6 d in acetate buffer (0.1 M, pH 4.7) or in 18.2 MΩ water. The samples were analyzed immediately after the start of incubation and after 3, 6, 24 h, 2, 3, and 6 d. For the protein interaction experiments HEWL (140 µM) and **1** (1 : 10) were incubated for 4 weeks and the samples were analyzed immediately after the start of incubation and after 1, 7, and 28 d. Both studies were conducted with a Bruker micrOTOF-Q II mass spectrometer in positive ion mode after 1 : 10 dilution of the samples with 30% acetonitrile/water containing 1% formic acid just before analysis. The Data Analysis 4.0 software package from Bruker Daltonics (Bremen, Germany) was used for processing of the data sets.

Table S2. Crystal data, collection, phasing and refinement.

	3 d	1 month
PDB ID	6BO1	6BO2
Data collection	AS MX1	AS MX1
Space group	$P4_32_12$	$P4_32_12$
Cell dimensions a, b, c (Å)	a = b = 78.1, c = 37.3	a = b = 78.8, c = 36.9
Wavelength (Å)	0.9537	0.9537
Unique reflections	33258	19993
Resolution range (Å)*	39.04-1.24 (1.26-1.24)	39.38-1.48 (1.50-1.48)
Rpim (%)*	0.02 (0.94)	0.02 (0.97)
I/σ(I)*	17.7 (0.7)	20.7 (0.8)
CC(1/2)*	0.999 (0.403)	0.999 (0.303)
Completeness (%)*	100.0 (99.9)	100.0 (99.3)
Multiplicity*	14.0 (13.1)	11.8 (10.6)
Phasing (MR Phaser)		
LLG	6282	1856
Z-score	61.7	42.1
Refinement		
Resolution (Å)	1.24	1.48
Rwork/Rfree (%)	0.20/0.23	0.19/0.23
No. atoms (residues)		
Protein	1036 (129)	1017 (129)
Water	119	78
Sodium	1	1
Ligands - site I	14 (1)	14 (1)
- site II	-	14 (1)
- site III	-	2 (2)
B-factors (Å^2)		
Wilson	14.3	19.3
Protein	20.5	29.7
Water	35.9	41.5
Ligand - site I	26.7 (0.65 occupancy)	34.6 (0.90 occupancy)
- site II	-	36.9 (0.80 occupancy)
- site III	-	31.6 (0.50 occupancy)
R.M.S. deviations		
Bond lengths (Å)	0.01	0.01
Bond angles (∘)	1.50	1.50

* Data for the outer shell data are shown in parenthesis.

Table S3. Literature analysis of binding sites identified for Ru compounds on HEWL.

PDB ID / reference	Complexes	Binding site(s)	Crystallisation method	Concentration / incubation ratios
5OB6[15]	*fac*-[$Ru^{II}(CO)_3Cl_2$(imidazole)]	His15 – $Ru(CO)_3(H_2O)_2$ (occ = 0.8) Asp18 – $Ru(H_2O)_4(CO)$ (occ = 0.5) Asp52 – $Ru(H_2O)$ (A conformer, occ = 0.3) Asp52/Asn46 – Ru (B conformer, occ = 0.3) Asp119/Arg125 – $Ru(CO)_2$ (occ = 0.5) C term (Leu129) – $Ru(H_2O)_3$ (occ = 0.3)	co-crystal, 1 d	protein : metal 1 : 10
5OB7[15]	*fac*-[$Ru^{II}(CO)_3Cl_2$(imidazole)]	His15 – $Ru(CO)_3(H_2O)Cl$ (occ = 0.8) Asp18 – $Ru(H_2O)_3(CO)_2$ (occ = 0.5) Asp119/Arg125 – $Ru(H_2O)$ (occ = 0.3)	co-crystal, 1 d	protein : metal 1 : 10
5OB8[15]	*fac*-[$Ru^{II}(CO)_3Cl_2$(Me-imidazole)]	His15 – $Ru(CO)_2(H_2O)_2Cl$ (occ = 0.8) Asp18 – $Ru(CO)(H_2O)_4$ (occ = 0.4)	co-crystal with NaCl as precipitant, 1 d	protein : metal 1 : 10
5OB9[15]	*fac*-[$Ru^{II}(CO)_3Cl_2$(Me-imidazole)]	His15 – $Ru(CO)_2(H_2O)_2$ (occ = 0.4) Asp119/Gln121 – $Ru(CO)_3(H_2O)$ (occ = 0.6)	co-crystal with ethylene glycol/$NaNO_3$ as precipitant, 1 d	protein : metal 1 : 10
4W94[16]	$[Ru^{II}(CO)_3Cl_2]_2$	His15 – $Ru(CO)_2(H_2O)Cl_2$ (occ = 0.75) Lys13/C term (Leu129) – $Ru(H_2O)$ (occ = 0.3) Asp18 – $Ru_2(CO)_4Cl_3(H_2O)$ (occ = 0.5) Asp52 – $Ru(H_2O)_3$ (occ = 0.35) Asp101 – 2x Ru (occ = 0.1) Asp119 – RuCl (occ = 0.5) C term (Leu129) – $Ru(H_2O)$ (occ = 0.5)	soak, 1 d	5 mM
4W96[16]	$[Ru^{II}(CO)_3Cl_2]_2$	His15 – $Ru(CO)_2(H_2O)Cl_2$ (occ = 0.7) Asp18 – Ru_2Cl (occ = 0.5) Asp52 – $Ru(H_2O)_3$ (occ = 0.3) Asp101 – Ru_2 (occ = 0.3 and 0.1) Asp119 – RuCl (occ = 0.3) C term (Leu129) – 2x Ru (occ = 0.3 and 0.5)	soak, 1 d; followed by reaction with deoxy-myoglobin solution	5 mM
4UWN[17]	$[Ru^{II}(CO)_3Cl_2$(methionine sulfoxide)]	His15 – $Ru(CO)(H_2O)_4$ (occ = 1) Asp18 – $Ru(CO)(H_2O)_3$ (occ = 0.65) Asp52 – $Ru(H_2O)_3$ (occ = 0.5) Asp119 – $Ru(H_2O)_3$ (occ = 0.5)	soak, 1 d	50 mM

Table S3. Cont'd.

PDB ID / reference	Complexes	Binding site(s)	Crystallisation method	Concentration / incubation ratios
4UWU[17]	$[Ru^{II}(CO)_3Cl_2(pyridine)]$	His15 – $Ru(CO)(CO_2)(H_2O)_3$ (occ = 0.8) Asp18 – 2x $Ru(H_2O)_4$ (occ = 0.5) Asp52 – $Ru(CO)(H_2O)_2$ (occ = 0.4) Asp101 – $Ru(H_2O)_4$ and $Ru(H_2O)_3$ (occ = 0.7) Asp119 – $Ru(CO)(H_2O)_4$ (occ = 0.7)	soak, 1 d	50 mM
4UWV[17]	$[Ru^{II}(CO)_3Cl_2(pyridine)]$	His15 – $Ru(CO)(H_2O)_4$ (occ = 0.7) Asp101 – $Ru(H_2O)_4$ and $Ru(H_2O)$ (occ = 0.65)	soak, 1d	50 mM
2XJW[18]	*fac*-$[Ru^{II}(CO)_3(Cl)(H_2NCH_2CO_2)]$	His15 – $Ru(CO)_2(H_2O)_3$ (occ = 0.8) Asp18 – $Ru(CO)_2(H_2O)_3$ (both occ = 0.5) Asp52 – $Ru(CO)_2(H_2O)_3$ (occ = 0.4)	soak, 24 h	0.1 M
5E9R[19]	*fac*-$[Ru^{II}(CO)_3Cl_2$(Me-benzimidazole)]	His15 – $Ru(CO)_2(H_2O)_2Cl$ (occ = 0.8)	co-crystal, 2 h	protein : metal 1 : 10
5LVG	*cis*-$[Ru^{II}(DMSO)_4Cl_2]$	Arg14/His15 – $Ru(H_2O)_2Cl$ (occ = 0.8)	n/a	n/a
5LVH	*trans*-$[Ru^{II}(DMSO)_4Cl_2]$	Arg14/His15 – $Ru(H_2O)Cl$ (occ = 0.7)	n/a	n/a
4J1A[20]	AziRu, $Na[Ru^{III}$(pyridine)Cl_4(DMSO)]	Arg14/His15/Asp87 – $Ru(H_2O)_3Cl$ (occ = 0.3)	soak formed green crystal, a few hours	saturated solution
4J1B[20]	AziRu, $Na[Ru^{III}$(pyridine)Cl_4(DMSO)]	Arg14/His15/Asp87 – $Ru(H_2O)_4$ (occ = 0.5)	soak formed black crystal, a few days	saturated solution
5LVI	(Hisoquinoline)[*trans*-$Ru^{III}Cl_4$(DMSO)(isoquinoline)]	Arg14/His15 – RuCl (occ = 0.3)	n/a	n/a
5LVJ	indazolium [*trans*-$Ru^{III}Cl_4$(DMSO)(indazole)]	Arg14/His15 – $RuCl(H_2O)_2$ (occ = 0.3)	n/a	n/a
4NY5[21]	NAMI-A, imidazolium $[Ru^{III}$(imidazole)Cl_4(DMSO)]	Asp119 – $Ru(H_2O)_3$ (occ = 0.4) Asp101 – $Ru(H_2O)_4$ (occ = 0.4)	co-crystal	protein : metal 1 : 10

Table S3. Cont'd.

PDB ID / reference	Complexes	Binding site(s)	Crystallisation method	Concentration / incubation ratios
5KJ9[22]	$[Ru^{II}(cym)$(N-(4-(maleimidyl)phenyl)-pyridine-2-carbothioamide)Cl]Cl	solvent channel near Trp108 – Ru (occ = 0.5)	soak, 7 d	1.6 mM
5V4G[23]	$[Ru^{II}(cym)Cl_2]_2$	His15 – $Ru(cym)Cl_2$ (occ = 0.9) Asp101 – $Ru(cym)Cl_2Ru$ (occ = 0.5)	soak, 1 d	3.2 mM
5V4H[23]	$[Ru^{II}(cym)Br_2]_2$	His15 – $Ru(cym)Cl_2$ (occ = 0.7)	soak, 1 d	2.5 mM
1T3P[24]	$[Ru^{II}(cym)(H_2O)Cl_2]$	His15 – $Ru(cym)Cl_2$ (occ = 1)	soak, 2 d	n/a
3W6A	$[Ru^{II}(\eta^6$-benzene$)Cl_2]_2$	His15 – $Ru(\eta^6$-benzene$)Cl_2$ (occ = 0.6) Asp101 – Ru (occ = 0.2)	n/a	5 mM

References

1 D. Liebschner, P. V. Afonine, N. W. Moriarty, B. K. Poon, O. V. Sobolev, T. C. Terwilliger and P. D. Adams, *Acta Crystallogr. Sect. D*, 2017, **73**, 148.

2 T. C. Terwilliger, R. W. Grosse-Kunstleve, P. V. Afonine, N. W. Moriarty, P. D. Adams, R. J. Read, P. H. Zwart and L. W. Hung, *Acta Crystallogr. Sect. D*, 2008, **64**, 515.

3 L. Oehninger, M. Stefanopoulou, H. Alborzinia, J. Schur, S. Ludewig, K. Namikawa, A. Munoz-Castro, R. W. Koster, K. Baumann, S. Wolfl, W. S. Sheldrick and I. Ott, *Dalton Trans.*, 2013, **42**, 1657.

4 C. C. F. Blake, R. H. Fenn, L. N. Johnson, D. F. Koenig, G. A. Mair, A. C. T. North, J. W. H. Oldham, D. C. Phillips, R. J. Poljak, V. R. Sarma and C. A. Vernon, *How the structure of lysozyme was actually determined*, 2006.

5 N. P. Cowieson, D. Aragao, M. Clift, D. J. Ericsson, C. Gee, S. J. Harrop, N. Mudie, S. Panjikar, J. R. Price, A. Riboldi-Tunnicliffe, R. Williamson and T. Caradoc-Davies, *J. Synchrotron Rad.*, 2015, **22**, 187.

6 W. Kabsch, *Acta Crystallogr. Sect. D*, 2010, **66**, 133.

7 A. J. McCoy, R. W. Grosse-Kunstleve, P. D. Adams, M. D. Winn, L. C. Storoni and R. J. Read, *J. Appl. Crystallogr.*, 2007, **40**, 658.

8 G. N. Murshudov, A. A. Vagin and E. J. Dodson, *Acta Crystallogr. Sect. D*, 1997, **53**, 240.

9 P. Emsley and K. Cowtan, *Acta Crystallogr. Sect. D*, 2004, **60**, 2126.

10 M. Nayal and E. Di Cera, *J. Mol. Biol.*, 1996, **256**, 228.

11 R. J. Read and A. J. Schierbeek, *J. Appl. Crystallogr.*, 1988, **21**, 490.

12 M. J. Frisch, G. W. Trucks, H. B. Schlegel, G. E. Scuseria, M. A. Robb, J. R. Cheeseman, G. Scalmani, V. Barone, B. Mennucci, G. A. Petersson, H. Nakatsuji, M. Caricato, X. Li, H. P. Hratchian, A. F. Izmaylov, J. Bloino, G. Zheng, J. L. Sonnenberg, M. Hada, M. Ehara, K. Toyota, R. Fukuda, J. Hasegawa, M. Ishida, T. Nakajima, Y. Honda, O. Kitao, H. Nakai, T. Vreven, J. A. Montgomery, J. E. Peralta, F. Ogliaro, M. Bearpark, J. J. Heyd, E. Brothers, K. N. Kudin, V. N. Staroverov, R. Kobayashi, J. Normand, K. Raghavachari, A. Rendell, J. C. Burant, S. S. Iyengar, J. Tomasi, M. Cossi, N. Rega, J. M. Millam, M. Klene, J. E. Knox, J. B. Cross, V. Bakken, C. Adamo, J. Jaramillo, R. Gomperts, R. E. Stratmann, O. Yazyev, A. J.

Austin, R. Cammi, C. Pomelli, J. W. Ochterski, R. L. Martin, K. Morokuma, V. G. Zakrzewski, G. A. Voth, P. Salvador, J. J. Dannenberg, S. Dapprich, A. D. Daniels, Farkas, J. B. Foresman, J. V. Ortiz, J. Cioslowski and D. J. Fox, (2009), Wallingford CT.

13 N. W. Moriarty, R. W. Grosse-Kunstleve and P. D. Adams, *Acta Crystallogr. Sect. D*, 2009, **65**, 1074.

14 N. Cetinbas, M. I. Webb, J. A. Dubland and C. J. Walsby, *J. Biol. Inorg. Chem.*, 2010, **15**, 131.

15 N. Pontillo, G. Ferraro, L. Messori, G. Tamasi and A. Merlino, *Dalton Trans.*, 2017, **46**, 9621.

16 H. Tabe, K. Fujita, S. Abe, M. Tsujimoto, T. Kuchimaru, S. Kizaka-Kondoh, M. Takano, S. Kitagawa and T. Ueno, *Inorg. Chem.*, 2015, **54**, 215.

17 J. D. Seixas, M. F. A. Santos, A. Mukhopadhyay, A. C. Coelho, P. M. Reis, L. F. Veiros, A. R. Marques, N. Penacho, A. M. L. Goncalves, M. J. Romao, G. J. L. Bernardes, T. Santos-Silva and C. C. Romao, *Dalton Trans.*, 2015, **44**, 5058.

18 T. Santos-Silva, A. Mukhopadhyay, J. D. Seixas, G. J. L. Bernardes, C. C. Romão and M. J. Romão, *J. Am. Chem. Soc.*, 2011, **133**, 1192.

19 G. Tamasi, A. Merlino, F. Scaletti, P. Heffeter, A. A. Legin, M. A. Jakupec, W. Berger, L. Messori, B. K. Keppler and R. Cini, *Dalton Trans.*, 2017, **46**, 3025.

20 A. Vergara, G. D'Errico, D. Montesarchio, G. Mangiapia, L. Paduano and A. Merlino, *Inorg. Chem.*, 2013, **52**, 4157.

21 L. Messori and A. Merlino, *Dalton Trans.*, 2014, **43**, 6128.

22 M. Hanif, S. Moon, M. P. Sullivan, S. Movassaghi, M. Kubanik, D. C. Goldstone, T. Sohnel, S. M. F. Jamieson and C. G. Hartinger, *J. Inorg. Biochem.*, 2016, **165**, 100.

23 M. P. Sullivan, M. Groessl, S. M. Meier, R. L. Kingston, D. C. Goldstone and C. G. Hartinger, *Chem. Commun.*, 2017, **53**, 4246.

24 I. W. McNae, K. Fishburne, A. Habtemariam, T. M. Hunter, M. Melchart, F. Wang, M. D. Walkinshaw and P. J. Sadler, *Chem. Commun.*, 2004, 1786.